RSC Sustainability

ROYAL SOCIETY OF CHEMISTRY

PAPER

View Article Online
View Journal

Cite this: DOI: 10.1039/d6su00123h

Research on microencapsulation of polyphenols obtained from *Pseuderanthemum palatiferum* leaves as promising delivery systems for antioxidant and antibacterial applications

Dang Huynh Minh Tam,[abc] Nguyen Hoang Phung,[abc] Tran Nguyen Cam Nhung,[abc] Hoang Minh Nam,[abc] Mai Thanh Phong,[abc] Pham Hung Viet[d] and Nguyen Huu Hieu *[abc]

This research aimed to prepare microcapsules of polyphenols from *Pseuderanthemum palatiferum* (*P. palatiferum*) using sodium alginate and chitosan as wall materials, with *P. palatiferum* extract as the core material *via* ionic gelation. Ionic gelation parameters were investigated to achieve optimal encapsulation efficiency of the polyphenol content. Independent factors, including sodium alginate, chitosan, and calcium chloride concentration, were designed and optimized using the Box–Behnken design of response surface methodology. The physical and chemical features of microcapsules were characterized using SEM, FTIR, and TGA. The antioxidant activity of the microcapsules was tested using DPPH (2,2-diphenyl-1-picryl-hydrazyl-hydrate) scavenging assay, while antibacterial activity against *Escherichia coli* and *Staphylococcus aureus* was examined. The results showed that the optimal encapsulation efficiency reached 72.53% under conditions of 1.77% sodium alginate, 0.5% chitosan, and 0.5% calcium chloride concentration. Compared with the blank microcapsules, extract-loaded microcapsules exhibited higher water content and solubility, and a swelling ratio that was reduced by more than 4.5 times. The microcapsules had a dense and compact structure with spherical forms and an average size of 1.9 mm. The bioactive compounds from the extract can be preserved under different environmental conditions due to the protection of microcapsules. Extract-loaded microcapsules, exhibiting notable antioxidant and antibacterial capacities, have considerable potential for applications in the food and pharmaceutical fields.

Received 28th February 2026
Accepted 3rd May 2026

DOI: 10.1039/d6su00123h

rsc.li/rscsus

Sustainability spotlight

This study presents a sustainable approach for stabilising plant-derived polyphenols using green extraction and biodegradable biopolymers. Polyphenols from *Pseuderanthemum palatiferum* leaves were obtained by supercritical carbon dioxide extraction and encapsulated in alginate–chitosan microcapsules *via* ionic gelation, without toxic solvents or high energy input. The system enhances antioxidant and antibacterial performance while improving stability, offering a bio-based alternative to synthetic additives. These results support the preservation of medicinal plants and the development of environmentally responsible and circular bio-based materials for safer functional products.

1 Introduction

For centuries, many medicinal plants have been used as plant-based medicines to cure many different diseases. Species within the Acanthaceae family are predominantly employed in the management of disorders related to the respiratory, nervous, and reproductive systems, gastrointestinal and urinary tract ailments, and dermatological conditions. They possess notable phytochemicals that exhibit diverse biological activities, including antioxidant, antibacterial, anti-inflammatory, anti-nociceptive, hepatoprotective, and leishmanicidal effects.[1] *Pseuderanthemum palatiferum* (*P. palatiferum*), known as "Hoan

[a]*VNU-HCM, Key Laboratory of Chemical Engineering and Petroleum Processing (Key CEPP Lab), Ho Chi Minh City University of Technology (HCMUT), 268 Ly Thuong Kiet Street, Dien Hong Ward, Ho Chi Minh City, Vietnam. E-mail: nhhieubk@hcmut.edu.vn*

[b]*Faculty of Chemical Engineering, Ho Chi Minh City University of Technology (HCMUT), 268 Ly Thuong Kiet Street, Dien Hong Ward, Ho Chi Minh City, Vietnam*

[c]*Vietnam National University Ho Chi Minh City (VNU-HCM), Linh Xuan Ward, Ho Chi Minh City, Vietnam*

[d]*Key Laboratory of Analytical Technology for Environmental Quality and Food Safety Control, VNU Hanoi, 334 Nguyen Trai, Thanh Xuan, Hanoi, Vietnam*

Ngoc" in Vietnamese, belongs to the Acanthaceae family, and it is well known as one of the valuable herbal plants found and researched in recent years. It is located in forests and is a popular folklore medicine in Asian countries due to its ability to treat various ailments, including inflammation, cancer, diabetes, tumours, and high blood pressure. In addition to treating human diseases, the plant is used to treat diseases in livestock, such as diarrhea in pigs and dogs and cholera in chickens and ducks.[2] Leaves and roots are commonly used for these purposes. *P. palatiferum* leaves have been reported to contain β-sitosterol, stigmasterol, kaempferol, apigenin, salicylic acid, saponin, triterpenoid, amino acids such as lysine and methionine, and minerals.[3] Among these, phenolic chemicals and other bioactive components contribute to their therapeutic properties. According to previous research, the biological stability of these phenolic compounds reduced when they were stored for extended periods of time at high humidity and temperatures.[4] This is due to the hydrogen-donating nature of the phenolic hydroxyl groups. All these compounds are susceptible to oxidative polymerization and isomerization when exposed to adverse conditions.[5] These processes result in reduced solubility, diminished bioavailability, and increased sensitivity to environmental factors, restricting their practical applications.

A potential strategy to enhance the stability of bioactive components is coating them with substances using biopolymers.[5] Nanotechnological approaches are effective methods to control the release of bioactive compounds, reducing their toxicity and preventing the decrease in bioactivity. Nanoparticle-based formulations, including nanoparticles, microspheres, encapsulated systems, and liposomes of herbal extracts, offer many advantages. Encapsulation technology entraps essential plant compounds into capsules, which extends shelf life and facilitates transport and application.[6] An appropriate material for the coating is essential, where the selected materials should be biodegradable, environmentally friendly, chemically inert to the active substance, and capable of gradually and precisely releasing their contents into the surrounding environment.[4]

Materials for encapsulation are selected based on their chemical structures and natural availability. The preferable materials are polysaccharides such as alginates, carrageenan, agar, gums, starch, cellulose, pectin, chitosan, and their derivatives.[7] Sodium alginate (SA) is commonly utilised in the food, medicine, cosmetics, and agricultural industries due to its nontoxic, biodegradable, biocompatible, and gel-forming characteristics.[8] Sodium alginate is composed of β-(1-4)-*d*-mannuronic acid (M) and α-(1-4)-l-guluronic acid (G) monomers linked by glycosidic bonds in a straight-chain configuration. The free carboxylic groups of alginate can react with divalent or trivalent salts, such as Ca^{2+}, Cu^{2+}, or Fe^{3+}, to form cross-links between polymer chains.[9] During this process, known as ionotropic gelation, the droplets rapidly undergo gelation to form a hydrogel characterized by a solid three-dimensional network, resulting from interactions between negatively charged polymer chains and divalent metal ions present in the solution. The metal ions diffuse into the liquid droplets, initiating cross-linking from the exterior to the interior, thereby generating capsules that encapsulate the active agent. This cross-linking mechanism involves coordination between guluronate (G) units and divalent or trivalent cations connecting to carboxylate ($–COO^-$) and hydroxyl (–OH) functional groups in the alginate matrix, commonly described by the "egg-box" model.[8]

Alginate is regarded as an ideal material for encapsulation because of its durability and capacity to facilitate controlled release. However, high porosity in microbeads is observed during the ionotropic gelation process. This promotes rapid movement of water or other fluids into or out of their structure, which is a disadvantage for the encapsulation of hydrophilic materials. Therefore, cationic polyelectrolytes such as chitosan have been applied in combination with ionic gelation to address this weakness. Chitosan (CS) is commonly used as a coating agent due to its excellent solubility, biodegradability, and compatibility with biological systems.[10] Chitosan is a natural polymer that is widely available and can be easily produced by the deacetylation of chitin.[11] Some outstanding properties that can be considered are non-toxicity, biodegradability, biocompatibility, stability, and sterility, thus making chitosan a promising candidate for the encapsulation and controlled release of bioactive compounds. The interaction of positively charged chitosan with the negatively charged surface of the alginate particles enables the formation of a polyelectrolyte complex. Many different double-layer formulations of chitosan and alginate have been designed to investigate the protective function of microcapsules. The results showed that the shielding effect of microcapsules was observed when the bilayer structure of chitosan and alginate was employed.[10]

In this study, polyphenols from *P. palatiferum* extract (PPE) were embedded in microcapsules using sodium alginate and chitosan as wall materials *via* ionic gelation. The fabrication of microparticles was investigated to determine the effects of individual factors, including sodium alginate, chitosan, and calcium chloride concentration, and their interactions on the polyphenol encapsulation efficiency. The encapsulation efficiency (EE) was optimized using Box–Behnken Response Surface Methodology (RSM). Subsequently, the obtained PPE microcapsules (PPEMs) were characterised to assess the physicochemical properties, stability, and bioactivity of the encapsulated polyphenols. Moreover, a particular focus is placed on their potential antioxidant and antibacterial activities, highlighting their potential in food and therapeutic applications.

2 Materials and methods

2.1. Materials

Fresh *P. palatiferum* leaves were collected from a local garden in Ho Chi Minh City, Vietnam, as shown in Fig. 1. The Folin Ciocalteu reagent was purchased from Scharlab, Spain. Gallic acid was purchased from Xilong (China). Sodium alginate, ethanol, calcium chloride, sodium carbonate, and sodium citrate were of analytical grade. Chitosan powder (75% deacetylated) was purchased from S-Green company, Vietnam.

2.2. Preparation of *P. palatiferum* extract

Fresh leaves were dried at 50 °C to reach a constant weight, and then ground and sieved through a 40-mesh stainless steel sieve

Fig. 1 Fresh *P. palatiferum* leaves.

to ensure a uniform particle size of the powder. A weight of 3 ± 0.005 g of powder was loaded into a supercritical CO_2 system (Applied Separations, USA) for the extraction. All parameters, including temperature, pressure, pump flow rate, co-solvent rate, and extraction time, were selected based on our previous research with minor modifications.[12] The operating conditions were applied with a carbon dioxide flow rate of 2 L min^{-1}, a pressure of 349 ± 0.5 bar, a co-solvent rate of 14.6 mL g^{-1}, and a temperature of 60 ± 1.0 °C for 2 h. A fully automated CO_2 extraction system with continuous pressure and temperature regulation was applied. The material was packed into a 50 mL stainless steel extraction tube. Following extraction, supercritical CO_2 reverts to its gaseous phase through depressurization, and the ethanolic PPE samples were collected in a tightly closed bottle and stored at 4 °C until analysis.

2.3. Preparation of microcapsules by ionotropic gelation

The encapsulation procedure was conducted following an ionic gelation method with minor modifications, as shown in Fig. 2.[4] Sodium alginate (SA) was used as a hydrophilic polysaccharide carrier, and PPE served as the core material. Initially, an SA solution was prepared by dissolving SA powder in warm distilled water until completely dissolved. The SA solution was then mixed with PPE at a volume ratio of 2 : 1 (v/v) and homogenized using a magnetic stirrer to obtain a uniform, viscous core dispersion. For the coating solution, chitosan (1%, w/v) was dissolved in 1% (v/v) acetic acid. Subsequently, a calcium chloride solution was added to the chitosan solution and thoroughly mixed to obtain a homogeneous coating solution.

The two prepared solutions were used for the encapsulation process. The coating solution was maintained under constant stirring at 300 rpm. The core solution was extruded dropwise through a 21 G syringe needle into the coating solution at a fixed distance of 20 cm between the needle tip and the surface of the solution. This distance allowed the droplets to form spherical beads before they came into contact with the surface of the coating solution, thereby preventing tail formation and bead deformation. The formed capsules remained in the solution for 30 min to ensure ionic crosslinking and complete solidification. The microcapsules were separated by filtration through Whatman no. 4 filter papers, washed with distilled water, and stored in sealed containers at −20 °C. The prepared capsules were freeze-dried overnight using a bench-scale freeze dryer (Vertical Freeze Dryer BK-FD12, BIOBASE, China) and stored in airtight containers until further analyses.

2.4. Optimization of microencapsulation conditions

The optimal encapsulation conditions for the polyphenol content in PPE were determined using the Box–Behnken experimental design (BBD) and response surface methodology. Table 1 displays three independent variables that were assessed at three levels (−1, 0, and +1) for range and levels, including sodium alginate concentration (*A*, 1–2%), chitosan concentration (*B*, 0.2–0.6%), and $CaCl_2$ concentration (*C*, 0.5–1.5%).

The model efficiently investigates the relationship between multiple factors and the desired responses. All experiments were conducted in an unplanned order to reduce the effects of uncontrolled variables that may introduce bias in the response. In the prediction of the optimum point, a second-order model

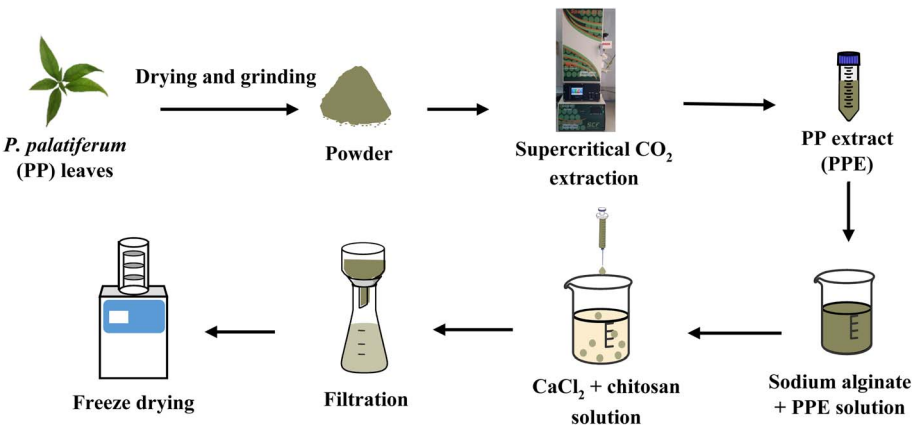

Fig. 2 The schematic preparation procedure of microcapsules.

Table 1 Variables of *P. palatiferum* extract microencapsulation parameters in Box–Behnken design

		Range and levels			
Independent variables	Symbols	−1	0	1	Dependent variable
SA concentration (%, w/v)	A	1	1.5	2	Y: EE (%)
CS concentration (%, w/v)	B	0.2	0.4	0.6	
$CaCl_2$ concentration (%, w/v)	C	0.5	1.0	1.5	

was fitted to correlate the relationship between independent variables and the response, which explains the variations caused by linear and second-order effects, as well as interactions. The relationship between the response values and independent variables was consistent with a quadratic polynomial model, according to eqn (1):

$$Y = b_0 + \sum_{1 \le j \le k} b_j X_j + \sum_{1 \le j \le l \le k} b_{jl} X_j X_l + \sum_i b_{jj} X_j^2 \quad (1)$$

where Y is the response variable to be modelled, b_0 is the constant coefficient, b_j is the linear coefficient, b_{jl} is the coefficient of an interaction effect, b_{jj} is the quadratic coefficient, X_j and X_l are the coded independent variables, and k is the number of independent parameters.

2.5. Determination of polyphenol content

The Folin–Ciocalteu assay was used to spectrophotometrically measure the polyphenol content in the leaf extract and microcapsules, using gallic acid as a standard.[13] The microcapsules (100 mg) were added to 10 mL of 5% (w/v) sodium citrate solution to disrupt the crosslinked network and release the encapsulated polyphenols. 0.02 mL of the sample was added to 1.5 mL of distilled water, followed by the addition of 0.1 mL of the Folin–Ciocalteu reagent. The solution was mixed and left for five min in the dark. Then, 0.3 mL of 20% Na_2CO_3 was added, and the mixture was left to react at room temperature in the dark for 90 min. Distilled water was used as the blank. The absorbance was measured at 765 nm using a UV-vis spectrophotometer (GENESYS 50 Spectrophotometer, Thermo Fisher Scientific Inc.) and compared with that of gallic acid equivalents (GAE). The total phenolic content (TPC) was determined in milligrams of gallic acid equivalent (GAE) per gram of dried leaves (mg GAE per g).

2.6. Characterization of microcapsules

2.6.1. Encapsulation efficiency. The encapsulation efficiency was determined according to a previous study with minor modifications.[10] An aliquot of 10 mg microcapsules was dissolved in 5 mL of sodium citrate (5%, w/v) solution, vigorously stirred for 30 min, sonicated for 30 min, and centrifuged for 10 min at 2000 rpm. The retention of phenolics within the microcapsules was assessed by calculating the phenolic encapsulation efficiency using eqn (2):

$$\mathrm{EE}(\%) = \frac{\mathrm{TPC_e}}{\mathrm{TPC_i}} \times 100\% \quad (2)$$

where TPC_e is the total polyphenol content encapsulated in the capsules, and TPC_i is the total polyphenol content in the initial extract solution used for the encapsulation process.

2.6.2. Moisture content. The moisture content of microcapsules was measured according to a previous study[14] with partial modification. A weight of 0.5 g of microcapsules was dried in an oven at 105 °C until a constant weight was reached. The moisture content of the microcapsules was calculated as the percentage of the mass difference between the samples before and after drying divided by the mass of the samples before drying.

2.6.3. Water solubility. Water solubility of microcapsules was determined following a previous study with small modifications.[14] Briefly, 0.3 g of microcapsules was dissolved in 20 mL of distilled water and stirred at 500 rpm for 30 min. Subsequently, the mixture was centrifuged, and the supernatant was transferred to a beaker and dried in an oven at 105 °C until a constant weight was reached. Water solubility was calculated as a percentage of the weight of the dried supernatant relative to the weight of the initial microcapsule sample.

2.6.4. Swelling properties. The swelling behaviour of the PPEM was investigated according to a previous method with minor modifications.[15] The microcapsule sample of 0.3 g was weighed and immersed in a glass vial containing distilled water at room temperature. The swollen spheres were weighed after the removal of excess water by filtration through a 60-mesh sieve. The investigation was conducted at 30 min intervals from 0 to 240 min, and the swelling ratio was determined using eqn (3).

$$\text{Swelling degree}(\%) = \frac{W_s - W_d}{W_d} \times 100\% \quad (3)$$

where W_s is the weight of the swollen sample and W_d is the weight of the initial dried sample.

2.6.5. Determination of the microcapsule size. The freeze-dried microcapsules were measured using a digital vernier caliper (Mitutoyo, USA).[16] A hundred beads were randomly selected from the sample, and the diameter was determined in triplicate.

2.6.6. Fourier transform infrared spectroscopy analysis. A Fourier transform infrared (FTIR) spectrometer (Bruker, MA, USA) was used to identify the functional groups, and FTIR spectroscopy confirmed the crosslinking between alginate and chitosan. Spectra were collected in the range of 4000–400 cm^{-1} at a resolution of 4 cm^{-1}, with 20 scans per sample. Background spectra were recorded prior to each measurement under

identical conditions. All measurements were conducted at room temperature.

2.6.7. Microcapsule morphology. The morphology of the freeze-dried microcapsules was observed with scanning electron microscopy (SEM) on an S-2400, Hitachi Instrument (California, USA) at an accelerating voltage of 10 and 15 kV.

2.6.8. Thermogravimetric analysis. Thermogravimetric analysis (TGA) was applied to test the thermal stability and decomposition of the microcapsules using a TGA instrument (STA PT 1600, Linseis GmbH, Germany). TGA was conducted under argon conditions in the temperature range of 30–600 °C with a heating rate of 10 °C min^{-1}.

2.7. *In vitro* polyphenol release study

The *in vitro* release of the polyphenol content from the microcapsules was investigated following a previous study with slight modifications.[17] The PPE microcapsules (100 mg) were suspended in two separate beakers containing 10 mL of hydrochloric acid solution (pH 1.2) and 10 mL of phosphate buffer solution (PBS, pH 7.4), respectively. The suspension was stirred at 200 rpm at a constant temperature of 37 °C (human body temperature). At 30 min intervals, 1 mL from each beaker was withdrawn from the solution and replaced with an equivalent volume of fresh media. The polyphenol content was determined spectrophotometrically at a wavelength of 765 nm using a UV-vis spectrophotometer (GENESYS 50 Spectrophotometer, Thermo Fisher Scientific Inc). The cumulative release was plotted *versus* time for each experiment, which was conducted in triplicate. The percentage of cumulative polyphenol release from the microcapsules was calculated as the ratio of TPC release divided by the initial TPC in the microcapsules.

2.8. Antioxidant properties

The free radical scavenging activity of microcapsules containing PPE was evaluated using the 2,2-diphenyl-1-picrylhydrazyl (DPPH) radical following the methodology outlined with minor modifications.[4,18,19] Briefly, microcapsules were dissolved in 30 mL of a mixture of ethanol : water : acetic acid (E : W : A) (50 : 42 : 8, v/v/v). The mixture was vigorously mixed for an hour and centrifuged at 2000 rpm for 10 min after sonicating for 30 min.

Aliquots of the supernatant were then diluted with methanol and prepared at different concentrations. A mixture of 4 mL of 0.076 mM DPPH solution was dissolved in methanol. The sample was mixed with DPPH solution, shaken, and then incubated at room temperature in the dark for 30 min. A spectrophotometer was used to measure the absorbance at 517 nm. An ascorbic acid solution was prepared at different concentrations as a reference standard. The percentage of DPPH radical scavenging activity was determined using eqn (4).

$$\text{Inhibition}(\%) = \frac{A_{\text{DPPH}} - A_{\text{Sample}}}{A_{\text{DPPH}}} \times 100 \quad (4)$$

where A_{DPPH} denotes the absorbance measurement of the DPPH control solution, while A_{Sample} represents the absorbance measurement of the DPPH solution in the presence of the leaf extract. All measurements were conducted in triplicate to ensure reliability.

2.9. Antibacterial properties

The antibacterial activities of the extract against Gram (−) *Escherichia coli* (*E. coli*) and Gram (+) *Staphylococcus aureus (S. aureus*) were determined using the disc diffusion method, with slight modifications.[18–20] Briefly, microcapsules were dissolved in 30 mL of a mixture of E : A : W (50 : 8 : 42, v/v/v). The mixture was vigorously mixed for an hour and centrifuged at 2000 rpm for 10 min after sonicating for 30 min. The media were prepared with Mueller–Hinton agar, autoclaved, cooled, poured into sterile Petri dishes, and allowed to solidify. Next, wells were created for the bacterial cultures. The bacterial suspension of 10^6 CFU mL^{-1} was swabbed evenly on the surface using a sterile swab. A small well with a 6 mm diameter was sterilised and impregnated with 100 μL extract, which was diluted in 10% dimethyl sulfoxide (DMSO). The incubation was conducted at 37 °C for 24 h. The diameters (mm) of the inhibition zones were measured, and the antibacterial activity values were represented as the mean of the inhibition zones (mm) from three replicates. Gentamicin (Ge) (20 μg mL^{-1}) was chosen to be a positive control, and an ethanol : water : acetic acid mixture was used to subtract the inhibition zone of encapsulated microcapsules.

2.10. Statistical analysis

All obtained data from the response surface design experiment were analysed using Design Expert software (version 11, StatEase Inc., Minneapolis, USA). The accuracy of the model was determined by the coefficient of determination R^2. Statistical analysis of the data was performed using SPSS (IBM SPSS Statistics 22) and then graphed using R and OriginPro 2024 software. The significant difference between the experiment data sets was determined using the statistical method of one-way ANOVA and the least significant difference (LSD) with $\alpha = 0.05$. The data from individual experiments were obtained in triplicate. All data are displayed as the mean ± standard deviation.

3. Results and discussion

3.1. Effect of factors on the polyphenol encapsulation efficiency

3.1.1. Single factor experiments on the polyphenols from extract. The polyphenol content in PPE can be effectively protected by encapsulation within sodium alginate capsules, which are biodegradable and nontoxic polymers. The encapsulation efficiency (EE) of polyphenols was used to evaluate the influence of individual formulation parameters, as presented in Fig. 3. Fig. 3A presents the influence of SA concentration when other parameters were fixed at chitosan and calcium ion concentrations of 0.4 and 1.5%, respectively. The EE of polyphenols increased slightly with the increase in SA concentration from 1 to 2%, reaching a maximum value of 58.10% at 2% SA. A higher SA concentration likely promotes the formation of a denser

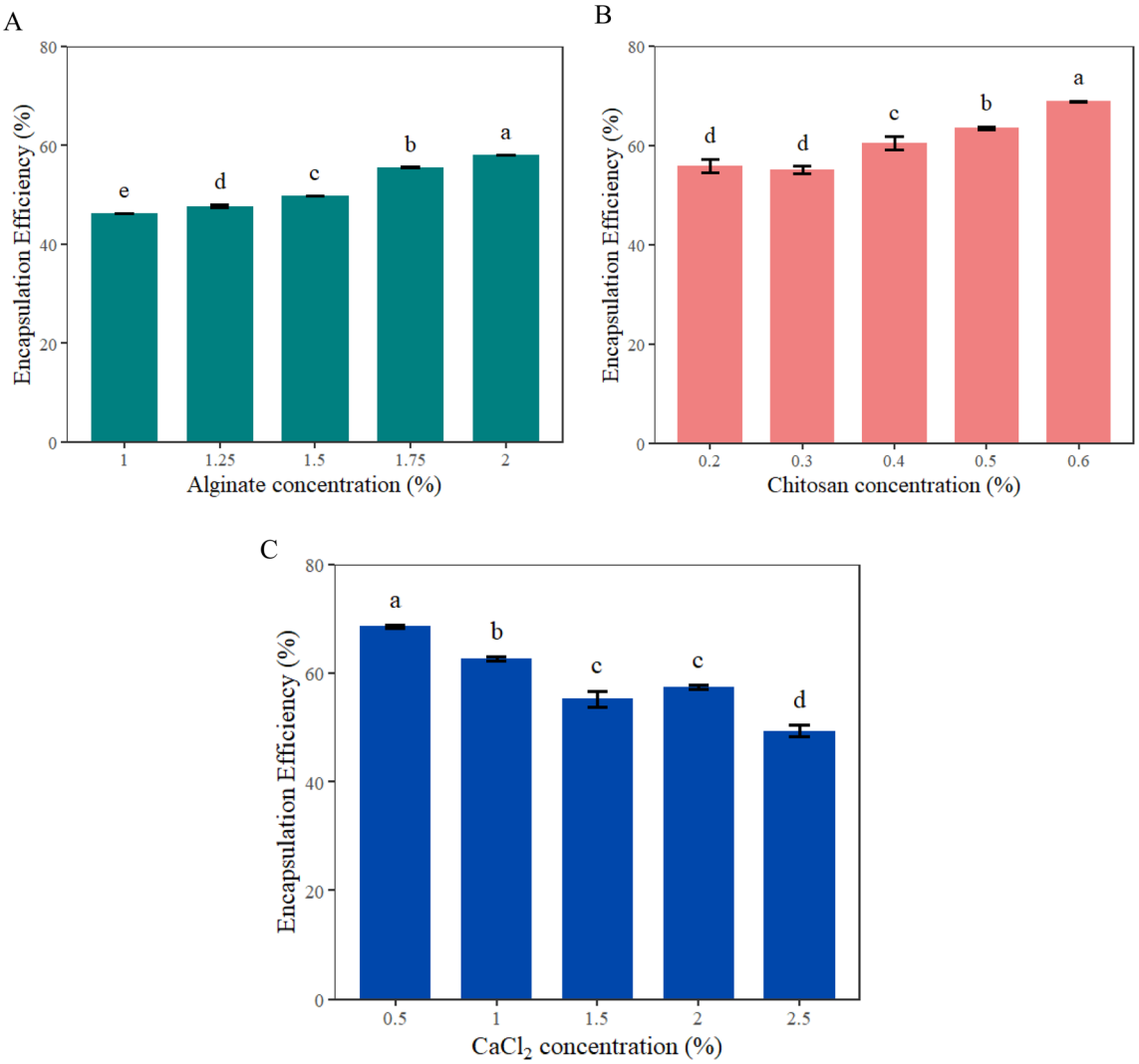

Fig. 3 The influences of alginate (A), chitosan (B), and $CaCl_2$ (C) concentration on the encapsulation efficiency. Different lowercase letters indicate significant differences ($p < 0.05$).

polymeric network, resulting in more compact capsules and improved retention of polyphenols.[21]

The effect of CS concentration on encapsulation efficiency was investigated in a set of 2% SA and 1.5% $CaCl_2$ concentration, as shown in Fig. 3B. The EE exhibited a similar value between 0.2 and 0.3% concentrations, and then slightly increased until it peaked at 68.879% at the highest chitosan concentration of 0.6%. The increase in EE with higher chitosan concentration may be attributed to the reinforcement of the outer polyelectrolyte layer, which enhances the structural integrity of the capsules and reduces polyphenol leakage. Fig. 3C shows the effect of calcium chloride concentration on the EE of polyphenols. When other conditions were set at 2% SA and 0.6% CS concentrations, the EE achieved the highest value of 68.6% at 0.5% $CaCl_2$ concentration. The excessive calcium ion content led to a decrease in EE, possibly due to the rapid crosslinking between alginate and calcium ions, which may hinder uniform network formation and result in structural defects within the capsules.[9,21]

3.1.2. Optimization of microcapsules by ionic gelation. Based on the investigated experiments, SA, CS, and $CaCl_2$ concentrations were used as independent factors for the polyphenol content in *P. palatiferum* leaves based on the BBD model, with the EE as the response value. A set of 17 experiments was then designed and conducted to determine the optimal conditions. The response surface experimental design and results are shown in Table 2. The polyphenol content showed notable variability under different extraction conditions, with the highest value observed at 68.654% at an SA concentration of 1.75%, CS concentration of 0.5%, and calcium chloride concentration of 1%.

The results of ANOVA are shown in Table 3. The F value for the model was 51.15 with $p < 0.0001$, indicating that the designed model for the extraction process is appropriate and significant. The lack of fit value had $p > 0.05$, and model incompatibility was insignificant, confirming that the model has provided adequate correlations between the independent variables and the response. The influence of $CaCl_2$

Table 2 Experimental results obtained by Box–Behnken design for polyphenol encapsulation efficiency

Experiments	SA concentration (%, w/v)	CS concentration (%, w/v)	$CaCl_2$ concentration (%, w/v)	EE (%)
1	1.5	0.5	1.5	54.878
2	1.5	0.4	1	59.297
3	2	0.5	0.5	68.397
4	1.75	0.5	1	68.228
5	1.75	0.5	1	68.654
6	2	0.6	1	49.102
7	2	0.4	1	51.584
8	2	0.5	1.5	45.050
9	1.75	0.6	1.5	46.545
10	1.75	0.5	1	66.950
11	1.75	0.5	1	66.101
12	1.75	0.5	1	68.390
13	1.5	0.5	0.5	63.850
14	1.5	0.6	1	55.048
15	1.75	0.4	1.5	50.959
16	1.75	0.4	0.5	63.421
17	1.75	0.6	0.5	66.681

concentration on the EE (%) was the greatest, followed by that of SA and CS concentrations. In addition, the interaction terms AC and BC, with all quadratic terms A^2, B^2, and C^2 had a vital effect on the efficiency ($p < 0.05$).

The regression coefficient R^2 and adjusted R^2 were 0.985 and 0.965, respectively. This indicated good fit, reliability, and effectiveness of the design equation. The determination coefficients (R^2) obtained from the analysis indicated a substantial correlation between the independent variables and the results. The ANOVA results provided an overall evaluation of the influence of various parameters on the polyphenol content. The final model equation for the quadratic mulple regression was obtained according to eqn (5).

$$Y = 67.67 - 2.37A - 0.9855B - 8.11C + 0.4418\mathrm{AB} - 3.59\mathrm{AC} - 1.92\mathrm{BC} - 6.38A^2 - 7.52B^2 - 3.24\mathrm{AC}^2 \quad (5)$$

Response surface graphs and contour maps of the three variables and their interactions are presented in Fig. 4. It can be observed from Fig. 4A and B that, when the SA concentration was constant, a tendency of increasing and then decreasing with increasing CS concentration was shown in EE (%). Conversely, at a constant CS concentration, a similar trend in EE (%) was observed with increasing SA concentration. At a fixed concentration of calcium chloride, the increase in SA formed a denser structure, leading to high encapsulation capability. However, the excessive CS concentration could hinder the cross-linking network between wall materials and calcium ions, thereby reducing the encapsulation efficiency.[21] Fig. 4C and D illustrate a simultaneous influence of SA and $CaCl_2$ concentrations on EE (%). At a high concentration of SA (2%) and a low concentration of $CaCl_2$ (0.5%), the highest encapsulation efficiency of 68.39% was obtained. When the SA concentration was unchanged, the EE (%) increased with decreasing concentrations of calcium ions, according to Fig. 4E and F. The influence of the calcium chloride concentration significantly affected EE (%), followed by that of sodium alginate and chitosan.

Table 3 ANOVA analysis results on polyphenol encapsulation efficiency

Source	Sum of squares	*df*	Mean square	*F*-value	*p*-value
Model	1147.17	9	127.46	51.15	<0.0001
A-SA concentration	44.84	1	44.84	17.99	0.0038
B-CS concentration	7.77	1	7.77	3.12	0.1208
C-$CaCl_2$ concentration	526.79	1	526.79	211.38	<0.0001
AB	0.7806	1	0.7806	0.3132	0.5932
AC	51.66	1	51.66	20.73	0.0026
BC	14.72	1	14.72	5.91	0.0454
A^2	171.54	1	171.54	68.83	<0.0001
B^2	238.42	1	238.42	95.67	<0.0001
C^2	44.18	1	44.18	17.73	0.0040
Residual	17.44	7	2.49		
Lack of fit	12.67	3	4.22	3.54	0.1268
Pure error	4.77	4	1.19		
Cor total	1164.62	16			

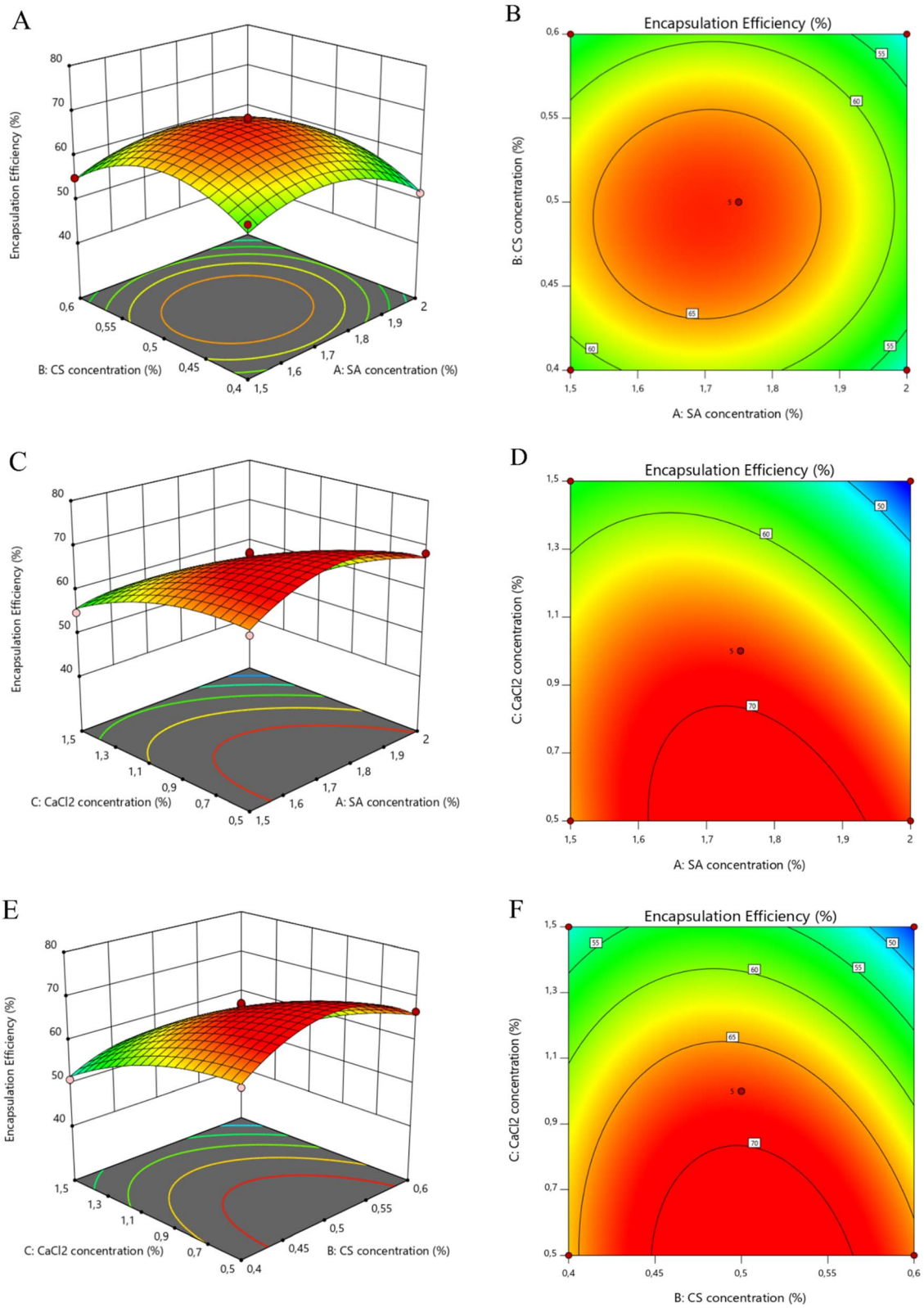

Fig. 4 Three-dimensional response surface graphs and contour maps for encapsulation efficiency as a function of SA concentration (A and B), CS concentration (C and D), and $CaCl_2$ concentration (E and F).

Verification of the proposed optimum conditions for polyphenol encapsulation efficiency is displayed in Table 4. The optimal results obtained by the equation model were SA, CS, and $CaCl_2$ concentrations of 1.774, 0.506, and 0.5%, respectively, with an EE of 72.632%. The optimal encapsulation conditions were determined at 1.77% SA, 0.5% CS, and 0.5%

Table 4 Verification experiments for the predicted and actual encapsulation efficiency values.

Optimal conditions			Predicted value	Experimental value	Average value	RSD (%)
A (%, w/v) 1.774	B (%, w/v) 0.506	C (%, w/v) 0.5	72.632	71.56 73.37 72.66	72.53	1.255

$CaCl_2$ concentrations, yielding an average EE of 72.53%. The dependent variable EE was predicted from RSM and compared with actual experimental values. Three replicates were conducted for the validation experiment under the optimized conditions to validate the model. The predicted (72.632%) and experimental (72.53%) EE values, with a relative standard deviation (RSD) value of 1.255%, confirmed the validity and reliability of the model.

3.3. Characteristics of microcapsules

3.3.1. Analysis of moisture content, swelling degree, solubility, and particle size. The moisture content, swelling degree, solubility of blank and PPE microcapsules, and particle size of beads after freeze drying are displayed in Fig. 5. The moisture content of blank microcapsules exhibited a slightly lower content of water than PPEMs, as shown in Fig. 5A. This might be attributed to the hydrophilic structure imparted by the polyphenol content in the extract, which interacts with water through hydrogen bonding. The increased number of hydroxyl groups in microcapsules promotes increased moisture retention in PPEMs.[22]

Biopolymers are known for their hydrophilicity and easy swelling in solution. The bioactive compounds that are embedded in microcapsules can be affected by their swelling properties in delivery and controlled release.[15] The swelling degree of microspheres was determined at intervals by comparing blank and extract-loaded samples. The microcapsules were tested in distilled water, where the solution pH was approximately 6, to simulate their application in other industries including food, medicine, and cosmetics. As shown in Fig. 5B, the swelling capacity of PPEMs gradually increased from over 1200% at 30 min to about 1600% at 240 min. In contrast, the swelling degree of blank microcapsules reached close to 2000% at 30 min and continued to increase steadily, reaching around 5700% at the end of the experimental period. The PPE microcapsules exhibited a notably lower swelling degree than the microcapsules without added extract. The high swelling index of the SA-CS co-polymer capsules reflects the hydrophilic properties of both wall materials at neutral pH.[23] The increase in extract concentration lowered the swelling index of the microcapsules, possibly because of the formation of intermolecular hydrogen bonds between the core and wall materials. This reduced the free space inside the capsules, leading to a restriction of water uptake. Furthermore, the protonated amino groups ($-NH_3^+$) of chitosan interact with the ionized carboxyl groups (–COO–) of alginate through electrostatic forces, resulting in the formation of a complex polyelectrolyte structure that inhibits the diffusion of water molecules into microcapsules.[17]

The water solubility of both blank and PPE microcapsules within 30 min was relatively low, at about 15.97 and 22.17%, respectively. As shown in Fig. 5C, the solubility trend was similar to the moisture content results, which might be attributed to the presence of polyphenols in the extract. The additional hydroxyl groups increased the solubility of PPE microcapsules due to the increased hydrogen bonding. As depicted in Fig. 5D, the extract-loaded microcapsules had an average size of 1.9 mm, with a range of particle size from 1.5 to 3 mm. The size of microcapsules was influenced by the size of the needle used in the experiment, which is displayed in Fig. 5E.

3.3.1. FTIR analysis. FTIR spectra were recorded to determine the interactions between different functional groups in the molecular structure of the sample. Fig. 6 shows the infrared spectra of PPE, blank microcapsules, and PPEMs. The FTIR spectrum showed a wide absorption band at around 3423 cm^{-1} attributed to the stretching vibration of –OH, which overlapped with the signal for the –NH bonding of the amino groups.[24] The encapsulated extract in sodium alginate microbeads formed hydrogen bonding between sodium alginate and polyphenol molecules, subsequently reducing the free –OH and weakening the band intensity. The absorption peak at 2929 cm^{-1} was attributed to the stretching vibration of CH_2 groups and could be associated with the presence of terpenes in the extract.[15] The sharp and intense absorption at 1631 cm^{-1} was indicative of the stretching vibration of C=O, which is attributed to the presence of undissociated carboxylic acid groups within the alginate film matrix.[9] The distinct peak at 1429 cm^{-1} was attributed to sodium alginate.[25] The peak at 1270 cm^{-1} represented aromatic C=C in the polyphenol from the extract, and the stretching vibration at 1055 cm^{-1} in the extract-loaded microcapsules also confirmed the presence of C–O.[15] The additional absorption band at 1152 cm^{-1} was possibly attributed to C–O–C stretching vibrations of saccharide compounds. Both peaks at 820 and 626 cm^{-1} are characteristic of out-of-plane C–H bending vibrations. The infrared spectra of the extract and microcapsules presented similar peaks, which showed that some of the main bioactive compounds in the extract were effectively encapsulated in the polymer matrix of microcapsules.

3.3.2. SEM analysis. The morphology of microcapsules was examined by SEM, as shown in Fig. 7. The results showed rough surfaces, heterogeneous pore sizes, and uneven folding. Moreover, no cracks were observed in both blank and PPE microcapsules. Their appearance resulted from the water loss during lyophilization.[16] As shown in Fig. 7A, the non-spherical morphology of blank capsules exhibited a collapsed center,

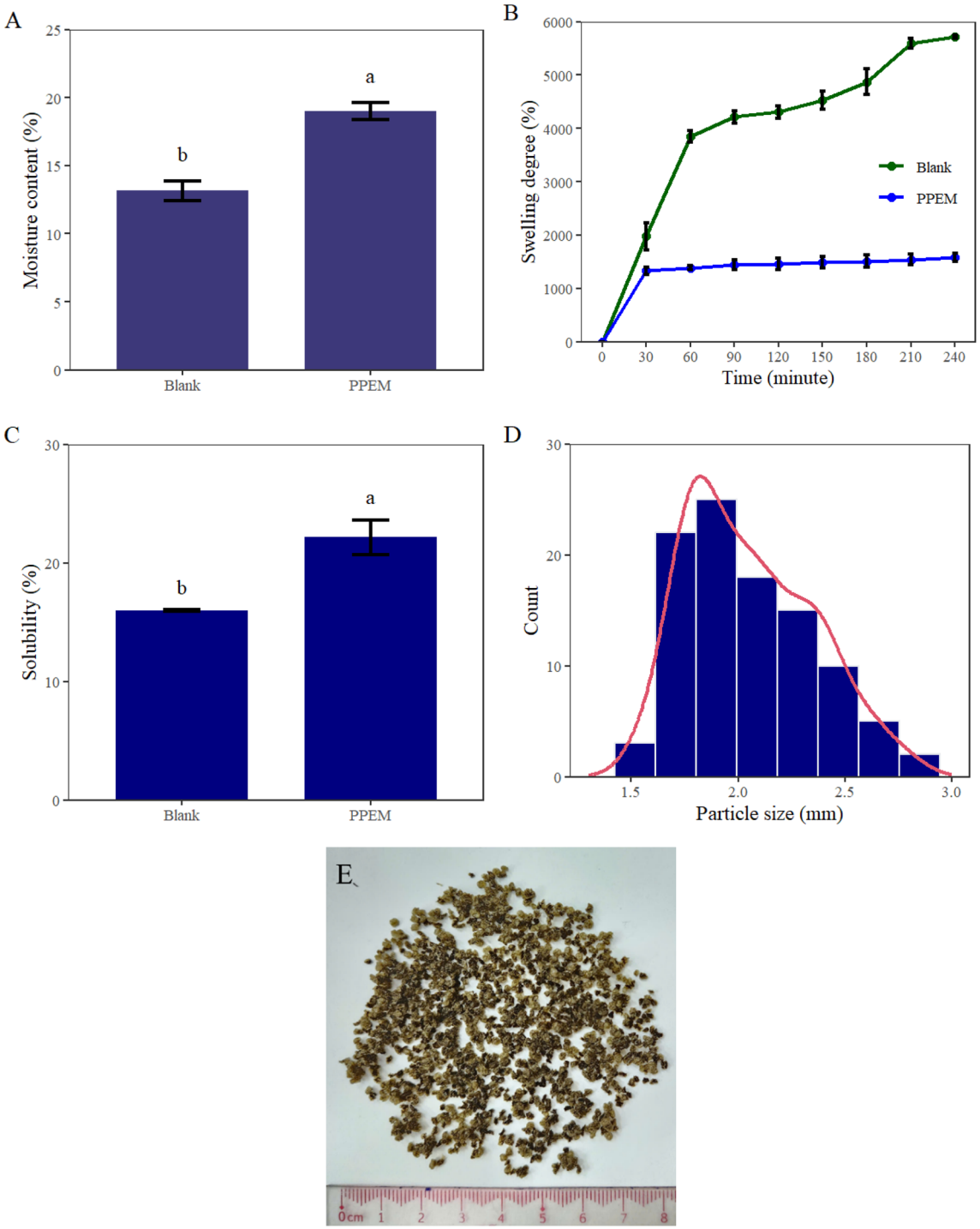

Fig. 5 The moisture content (A), swelling degree (B), solubility (C) of blank and PPE microcapsules, the PPEM size (D), and relative size of capsules prepared by a syringe (E). Different uppercase letters indicate a significant difference among samples.

a denser structure, and some large pores with folds. In contrast, a more intact shape, with regular spherical morphology, smaller pores, and a looser structure of PPEMs is observed in Fig. 7B. The crumpled appearance of blank capsules could be due to the sublimation of water during the drying process. The PPE microcapsules exhibited a rough surface with visible aggregates of the biopolymer blend and minor dents.

In addition, at a magnification of 5000 times as shown in Fig. 7C and D, the surface of the PPEM appeared as a stack of particles, whereas blank gel spheres appeared as a smooth and more uniform surface. The hydrogen bonds between polysaccharide chains resulted in a compact network and structural stability.[16] Additionally, the shrivelled surface is commonly attributed to the crosslinking of alginate and calcium

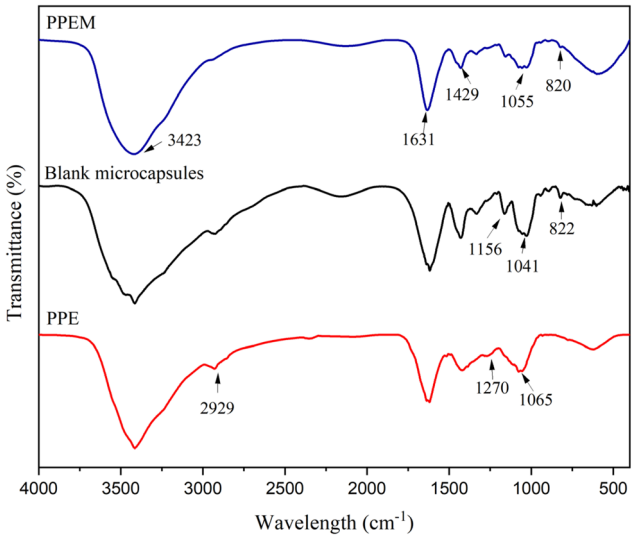

Fig. 6 FTIR spectra of PPE, blank microcapsules, and PPEMs.

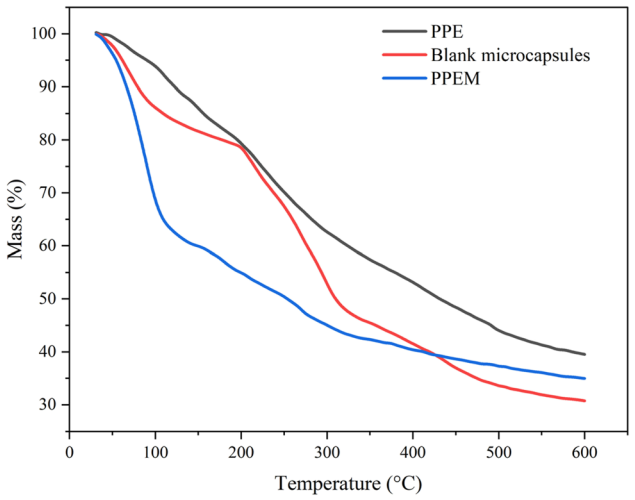

Fig. 8 TGA thermograms of blank microcapsules, PPE, and PPEMs.

chloride.[15] Alginate within the matrix formed a dense network of biopolymer chains, while the fibrous surface likely resulted from the formation of a polyelectrolyte complex between alginate and chitosan.[26] This compact structure of microcapsules is expected to effectively protect the internal material from the external environment, thus maintaining the bioactive compounds of the loaded extract.

3.3.3. Thermal stability analysis. The thermal behaviour of PPE microcapsules is depicted in Fig. 8 for analysing the thermal stability and decomposition of the capsules. The weight loss at the first stage, between 30 and 150 °C, was attributed to water evaporation. The weight losses of 14.10, 18.38, and 40.10% were recorded for PPE, blank, and PPEMs, respectively. Notably, the greater mass loss of PPEMs may be attributed to the higher moisture content of PPEMs, thereby resulting in the greatest loss of water. At the second stage, from 150 to 350 °C, the thermal degradation of PPEMs resulted in a loss of 15%, whereas that of the blank samples decreased by 36.15%. This stage was primarily attributed to the decomposition of polysaccharides, namely sodium alginate and chitosan, and other

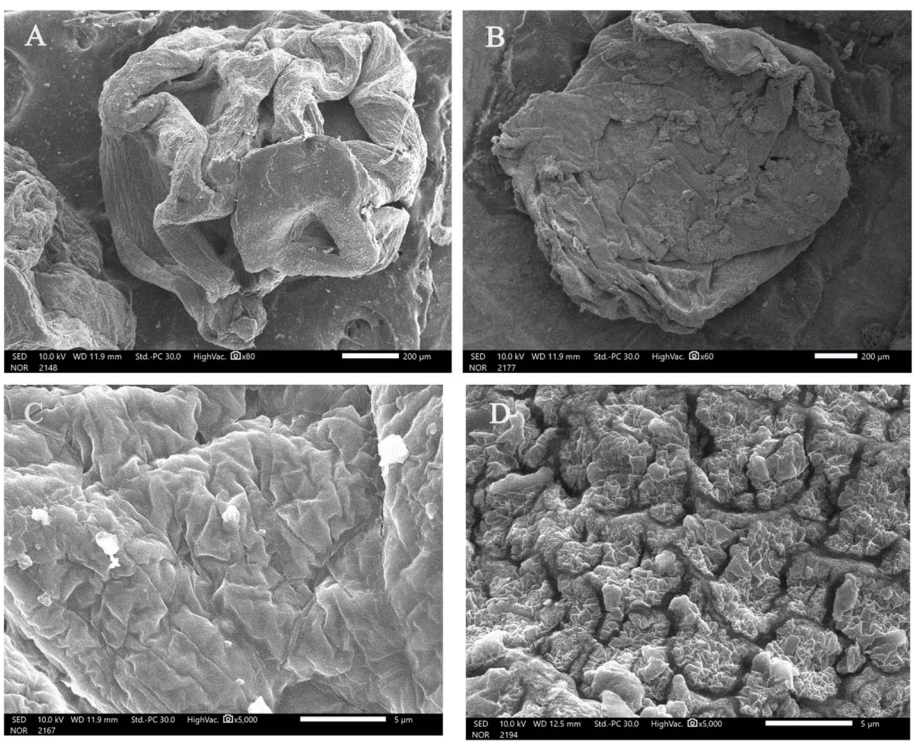

Fig. 7 SEM images of PPEMs and blank microcapsules at a magnification of 60 times (A and B) and PPEMs and blank microcapsules at a magnification of 5000 times (C and D).

macromolecules from wall materials.[27] During the third stage between 300 and 600 °C, PPEM and blank samples exhibited similar curves of mass reduction, with residual masses of 39.52 and 30.72%, respectively. A slight degradation of PPEMs was seen with a loss of about 10%. During this stage, the breakdown of biopolymers and carbon-rich residues was attributed to the continued thermal decomposition of wall materials. The thermal analysis patterns of microcapsules are consistent with those reported in previous studies.[9,22,28] The thermal stability of microcapsules suggests the possible protection of the loaded extract by outer materials, thereby easing the storage and transportation of food in diverse environments.

3.4. Polyphenol release from microcapsules

The extract release from microcapsules in simulated gastric acid (pH 1.2) and intestinal fluids (pH 7.4) is depicted in Fig. 9. A similar trend in cumulative release was observed in both environments, where the values substantially increased in the first 30 min, followed by a slight increase. At pH 1.2, there was a rapid initial release (47.7%) in the first interval, followed by a slight fluctuation and ongoing release (61.18%) at 300 min. In simulated intestinal solution, a very rapid release of 55.88% was observed after 30 min, and then it continued to increase until it achieved 90.44% release of polyphenols from PPEMs. When carboxyl groups from alginate were protonated in an acidic environment, they formed intermolecular hydrogen bonds that prevented the hydrogel network from swelling and breaking down in the stomach.[29] Moreover, the amino groups in chitosan were protonated and increased its affinity for the carboxyl groups in sodium alginate, thereby extending the swelling time.[30] Based on previous studies, the increase in the pH in the intestinal fluid weakened electrostatic repulsion between carboxyl groups, which led to the removal of protons. This accelerated the swelling of hydrogel spheres, which in turn caused the hydrogel network to collapse and decompose, ultimately resulting in the release of polyphenols in the intestines. Furthermore, the high affinity of phosphate ions in buffer solution induced disruption of the calcium-alginate gel matrix.[31] Similar trends have been reported in previous studies, where cumulative extract release from beads was significantly higher under alkaline conditions.[17,21,29,31]

3.5. Antioxidant activity

The free radical scavenging activity of the extract from both PPE and PPEMs against DPPH is presented in Fig. 10 and Table 5. The antioxidant activities of PPE and PPEMs were investigated at different concentrations ranging from 0 to 1400 μg mL^{-1}, and the results are presented as IC_{50} (50% inhibition concentration). The scavenging activity of PPE was 16.707% at 50 μg mL^{-1}, which consistently increased to 94.9% at 300 μg mL^{-1}. A concentration of 100 μg mL^{-1} of PPEMs scavenged 15.837% of free radicals. The DPPH scavenging activity of the extract loaded in microcapsules reached 97.156% at a concentration of 500 μg mL^{-1}. A large amount of PPE extract in the microcapsules was needed to nearly completely reduce the DPPH radical compared with that before encapsulation. In addition, the percentage of free radical scavenging of PPE was nearly 95% at 300 μg mL^{-1}, while PPEMs scavenged about 60.6%. The DPPH scavenging activity of the PPEM was consistently lower than that of the PPE. The observed antioxidant activity is primarily due to phenolic hydroxyl groups and other redox-active phytochemicals present in the leaf extract, which promote free radical neutralization.[18,19] Furthermore, the percentage of DPPH radical-scavenging activity was slightly lower than that of the bioactive compounds encapsulated in the microcapsules. This observation could be accounted for by encapsulation that resulted in a polymeric layer and a strong interaction between the extract and wall materials. Therefore, the amount of obtained bioactive compounds was lower than the initial feed.[32]

In the comparison with vitamin C in terms of IC_{50}, an amount of 7.166 μg mL^{-1} of vitamin C inhibited 50% of the free radical DPPH. In contrast, the values of 148.47 μg mL^{-1} for PPE and 249.698 μg mL^{-1} for PPEMs were observed. Vitamin C is widely recognized for its effectiveness as an antioxidant. The

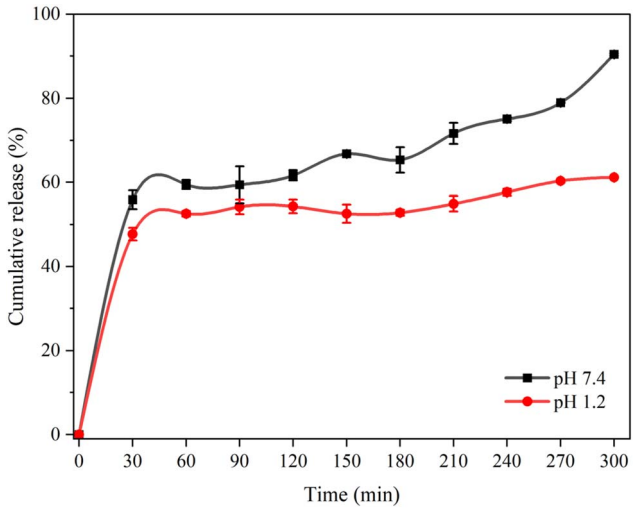

Fig. 9 Cumulative release of PPE microcapsules at pH 1.2 and 7.4.

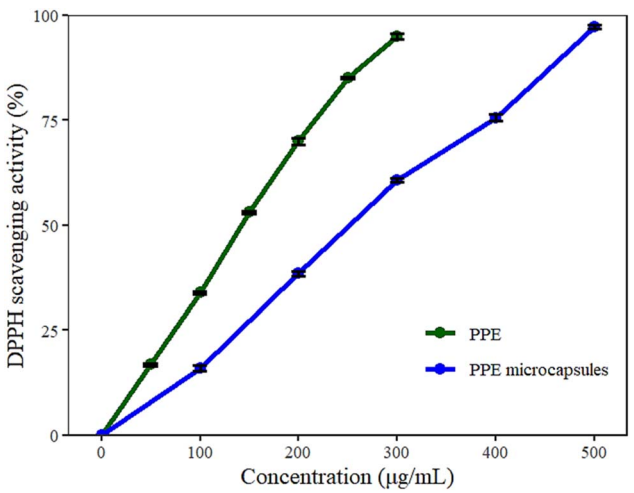

Fig. 10 Antioxidant properties of PPE and PPEMs.

Table 5 Inhibitory activity of PPE and PPEMs on the DPPH radical

Samples	IC_{50} (μg mL^{-1})
Vitamin C	7.166 ± 0.009
PPE	148.470 ± 0.929
PPEM	249.698 ± 0.979

antioxidant properties of the extract from both extraction methods were lower than those of vitamin C in overall effectiveness. The extract from *P. palatiferum* leaves has slightly significant antioxidant activity due to the presence of flavonoids and phenolic components in the total polyphenol content. These bioactive compounds have the capacity to scavenge free radicals, which demonstrates antioxidant activity. It has been proposed that oxidative stress is involved in the pathophysiology of many chronic and neurodegenerative diseases, and antioxidant treatment shows promise as a potential therapeutic strategy. Through three different ways of scavenging radicals, speeding up their breakdown, or stopping their production, these compounds shield cells from damage caused by free radicals.[33]

3.5. Antibacterial activity

The antibacterial effects of the extract from both PPE and PPEMs on *E. coli* and *S. aureus* are displayed in Fig. 11. A clear inhibitory zone was observed against two types of bacteria, including Gram-positive and Gram-negative. The extract displayed a similar inhibitory effect on both bacterial strains. In addition, after subtracting the effect of the E : A : W mixture from PPEMs, the results confirmed that the mixture exhibited antimicrobial activity. These findings demonstrated that the encapsulated polyphenols inhibited the growth of the bacterial strains. The smaller inhibition zone of the PPEM is related to the method of obtaining the extract inside capsules, which results in a reduced amount of polyphenols. The disruption of cell membrane integrity appears to be the initial step in the mechanism of exerting bacteriostatic action. Leaf extract and its encapsulated capsules are believed to promote bacterial death by inducing cell membrane damage based on bioactive ingredients containing lipophilic and hydrophobic functional groups. This activity is commonly observed against many pathogenic microorganisms.[18,19] These compounds interact with cell membranes, leading to leakage of intracellular components including proteins, nucleic acids and some essential molecules.[32] It is suggested that the mode of inhibitory action of PPE and PPEMs on *S. aureus* may occur directly through disruption of the structure of the cell membrane, leading to a loss of cell viability. These results suggest that the microcapsules loaded with PPE might have potential for clinical and food applications that require further study.[28]

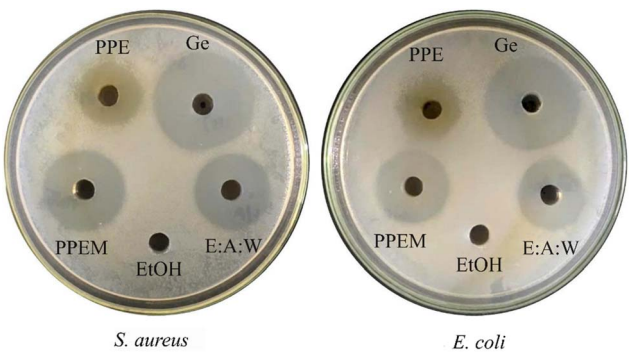

Fig. 11 Antibacterial properties of PPE and PPEMs against *S. aureus* and *E. coli*.

4 Conclusion

In this study, polyphenol content from *P. palatiferum* extract (PPE) was successfully encapsulated within a bilayer system of chitosan and sodium alginate using ionic gelation. The effects of sodium alginate (SA), chitosan (CS), and $CaCl_2$ concentrations on encapsulation efficiency were systematically evaluated through single-factor experiments and further optimized using response surface methodology (RSM) with a Box–Behnken design. The efficiency achieved was 72.53% under the optimized conditions with 1.77, 0.5, and 0.5% of SA, CS, and $CaCl_2$ concentrations, respectively, which was close to the anticipated result of 72.63%. The PPE microcapsules (PPEMs) exhibited desirable physicochemical properties, including controlled swelling behaviour, moderate solubility, and a spherical morphology. The FTIR and SEM results confirmed the intermolecular interactions between the core and polymer matrices. The thermal stability of microcapsules showed the possible protection of bioactive compounds. Biological activity analysis demonstrated that the antioxidant activity of PPE against DPPH free radicals was retained in the microcapsules. In addition, PPEMs inhibited both Gram-negative *Escherichia coli* and Gram-positive *Staphylococcus aureus*. These findings suggest that the PPEM has good performance in preserving bioactive substances, which is sufficient for further application in extending the shelf-life of food products. This research contributes to the microencapsulation of leaf extract and highlights its promising applicability in the food and pharmaceutical industries.

Author contributions

Dang Huynh Minh Tam: writing – original draft, formal analysis, conceptualization, methodology, visualization. Nguyen Hoang Phung: data curation, investigation, formal analysis. Tran Nguyen Cam Nhung: review and editing. Hoang Minh Nam: resources, writing – review & editing. Mai Thanh Phong: resources, writing – review & editing. Pham Hung Viet: investigation, writing – review & editing. Nguyen Huu Hieu: resources, supervision, writing – review & editing.

Conflicts of interest

The authors declare that they have no known competing financial interests or personal relationships that could have appeared to influence the work reported in this paper.

Data availability

The datasets generated during and/or analysed during the current study are available from the corresponding author upon reasonable request.

Acknowledgements

This research was funded by Vietnam National University Ho Chi Minh City (VNU-HCM) under grant number: B2024-20-35. We acknowledge the Ho Chi Minh City University of Technology (HCMUT), VNU-HCM for supporting this study.

References

1 E. A. Manzitto-Tripp, I. Darbyshire, T. F. Daniel, C. A. Kiel and L. A. McDade, Revised classification of Acanthaceae and worldwide dichotomous keys, *Taxon*, 2022, **71**(1), 103–153, DOI: 10.1002/tax.12600.

2 H. K. Dieu, C. B. Loc, S. Yamasaki, and Y. Hirata, "The Ethnobotanical and Botanical Study on Pseuderanthemum palatiferum as a New Medicinal Plant in the Mekong Delta of Vietnam," 2005. [Online]. Available: https://www.jircas.affrc.go.jp.

3 T. C. Ho and B. S. Chun, Extraction of Bioactive Compounds from Pseuderanthemum palatiferum (Nees) Radlk. Using Subcritical Water and Conventional Solvents: A Comparison Study, *J. Food Sci.*, 2019, **84**(5), 1201–1207, DOI: 10.1111/1750-3841.14501.

4 E. Kurtulbaş, R. Albarri, M. Torun and S. Şahin, Encapsulation of Moringa oleifera leaf extract in chitosan-coated alginate microbeads produced by ionic gelation, *Food Biosci*, 2022, **50**, 102158, DOI: 10.1016/j.fbio.2022.102158.

5 C. Chen *et al.*, *Advances in Oligosaccharides and Polysaccharides with Different Structures as Wall Materials for Probiotics Delivery: A Review*, Elsevier B.V., 2024, DOI: 10.1016/j.ijbiomac.2024.134468.

6 G. Diana, *et al.*, Chitosan for improved encapsulation of thyme aqueous extract in alginate-based microparticles, *Int. J. Biol. Macromol.*, 2024, **270**, 132493, DOI: 10.1016/j.ijbiomac.2024.132493.

7 A. Xie *et al.*, *Polysaccharides, Proteins, and Their Complex as Microencapsulation Carriers for Delivery of Probiotics: A Review on Carrier Types and Encapsulation Techniques*, Elsevier B.V. 2023, DOI: 10.1016/j.ijbiomac.2023.124784.

8 S. Swarupa and P. Thareja, *"Techniques, Applications and Prospects of Polysaccharide and Protein Based Biopolymer Coatings: A Review," May 01, 2024*, Elsevier B.V., DOI: 10.1016/j.ijbiomac.2024.131104.

9 L. Deng, *et al.*, Calcium alginate-encapsulated propolis microcapsules: Optimization, characterization, and preservation effects on postharvest sweet cherry, *Int. J. Biol. Macromol.*, 2024, **282**, 137473, DOI: 10.1016/j.ijbiomac.2024.137473.

10 L. E. N. Castro, *et al.*, Application of functional compounds from agro-industrial residues of Brazilian's tropical fruits extracted by sustainable methods in alginate-chitosan microparticles, *Bioact. Carbohydr. Dietary Fibre*, 2024, **32**, 100441, DOI: 10.1016/j.bcdf.2024.100441.

11 S. O. Olunusi, N. H. Ramli, F. Adam, E. Hossain, and T. H. Kim, *Chitosan as a Sustainable Alternative for Fresh Food Packaging: Structural Insights, Modification Strategies, and Innovations for Commercial Viability*, Elsevier B.V., 2025, DOI: 10.1016/j.ijbiomac.2025.145065.

12 D. P. M. Huong, *et al.*, Synthesis of biodegradable chitosan film loaded with Pseuderanthemum palatiferum leaf extract obtained by supercritical CO2 extraction: Characterization, antibacterial properties, and fruit preservation, *J. Supercrit. Fluids*, 2026, **227**, 106736, DOI: 10.1016/j.supflu.2025.106736.

13 D. T. Ayele, M. L. Akele and A. T. Melese, Analysis of total phenolic contents, flavonoids, antioxidant and antibacterial activities of Croton macrostachyus root extracts, *BMC Chem.*, 2022, **16**(1), 30, DOI: 10.1186/s13065-022-00822-0.

14 Q. Chen, C. Zhao, X. Ma, W. Yan and F. Wang, Preparation and characterization of walnut oil microcapsules by complex coacervation with sodium alginate and chitosan, *LWT*, 2025, **222**, 117630, DOI: 10.1016/j.lwt.2025.117630.

15 Q. Liu, Y. Li, R. Han, X. Zhuansun, L. Wang and H. Chen, Sodium alginate/gelatin hydrogel spheres loaded with Fructus Ligustri Lucidi essential oil: Preparation, characterization and biological activity, *Int. J. Biol. Macromol.*, 2024, **272**, 132726, DOI: 10.1016/j.ijbiomac.2024.132726.

16 Y. Sun, et al., Co-microencapsulation of Lactobacillus paracasei and Inonotus obliquus polysaccharide in alginate system: Physicochemical and functional properties, *Food Hydrocoll.*, 2025, **166**, 111344, DOI: 10.1016/j.foodhyd.2025.111344.

17 C. Dima, L. Pətraşcu, A. Cantaragiu, P. Alexe and Ş. Dima, The kinetics of the swelling process and the release mechanisms of Coriandrum sativum L. essential oil from chitosan/alginate/inulin microcapsules, *Food Chem.*, 2016, **195**, 39–48, DOI: 10.1016/j.foodchem.2015.05.044.

18 F. Ulusu and Y. Ulusu, Biosynthesis and Characterization of Silver Nanoparticles Mediated by Cistus salviifolius L. and Ferula communis L. Extracts and Evaluation of Their Antioxidant, Antibacterial, and Cytotoxic Potentials, *Biol. Bull.*, 2024, **51**(4), 845–856, DOI: 10.1134/S1062359023603634.

19 F. Ulusu, A. Sarilmaz, Y. Ulusu and F. Ozel, Quaternary nanorods: promising versatile agents for cancer therapy, antimicrobial strategies and free radical neutralization, *Part. Sci. Technol.*, 2024, **42**(6), 944–952, DOI: 10.1080/02726351.2023.2299869.

20 J. Oonmetta-aree, T. Suzuki, P. Gasaluck and G. Eumkeb, Antimicrobial properties and action of galangal (Alpinia galanga Linn.) on Staphylococcus aureus, *LWT*, 2006, **39**(10), 1214–1220, DOI: 10.1016/j.lwt.2005.06.015.

21 M. Yousefi, E. Khanniri, M. Shadnoush, N. Khorshidian and A. M. Mortazavian, Development, characterization and in vitro antioxidant activity of chitosan-coated alginate

microcapsules entrapping Viola odorata Linn. extract, *Int. J. Biol. Macromol.*, 2020, **163**, 44–54, DOI: 10.1016/j.ijbiomac.2020.06.250.

22 Y. Feng, C. Jin, S. Lv, H. Zhang, F. Ren, and J. Wang, *Molecular Mechanisms and Applications of Polyphenol-Protein Complexes with Antioxidant Properties: A Review*, Multidisciplinary Digital Publishing Institute (MDPI), 2023, DOI: 10.3390/antiox12081577.

23 O. F. Nwabor, S. Singh, D. Marlina and S. P. Voravuthikunchai, Chemical characterization, release, and bioactivity of Eucalyptus camaldulensis polyphenols from freeze-dried sodium alginate and sodium carboxymethyl cellulose matrix, *Food Qual. Saf.*, 2020, **4**(4), 203–212, DOI: 10.1093/fqsafe/fyaa016.

24 P. P. Nadira, V. M. A. Mujeeb, P. M. Rahman and K. Muraleedharan, Effects of cashew leaf extract on physicochemical, antioxidant, and antimicrobial properties of N, O–Carboxymethyl chitosan films, *Carbohydr. Polym. Technol. Appl.*, 2022, **3**, 100191, DOI: 10.1016/j.carpta.2022.100191.

25 T. Beldarrain-Iznaga, R. Villalobos-Carvajal, J. Leiva-Vega and E. Sevillano Armesto, Influence of multilayer mi;croencapsulation on the viability of Lactobacillus casei using a combined double emulsion and ionic gelation approach, *Food Bioprod. Process.*, 2020, **124**, 57–71, DOI: 10.1016/j.fbp.2020.08.009.

26 Y. Zhao, H. Li, Y. Wang, Z. Zhang and Q. Wang, Preparation, characterization and release kinetics of a multilayer encapsulated Perilla frutescens L. essential oil hydrogel bead, *Int. J. Biol. Macromol.*, 2023, **249**, 124776, DOI: 10.1016/j.ijbiomac.2023.124776.

27 K. Wang, *et al.*, Preparation and characterization of active films based on oregano essential oil microcapsules/soybean protein isolate/sodium carboxymethyl cellulose, *Int. J. Biol. Macromol.*, 2024, **258**, 128985, DOI: 10.1016/j.ijbiomac.2023.128985.

28 Z. Feyissa, G. D. Edossa, N. K. Gupta and D. Negera, Development of double crosslinked sodium alginate/chitosan based hydrogels for controlled release of metronidazole and its antibacterial activity, *Heliyon*, 2023, **9**(9), DOI: 10.1016/j.heliyon.2023.e20144.

29 Z. Li, Y. Geng, K. Bu, Z. Chen, K. Xu and C. Zhu, Construction of a pectin/sodium alginate composite hydrogel delivery system for improving the bioaccessibility of phycocyanin, *Int. J. Biol. Macromol.*, 2024, **269**, 131969, DOI: 10.1016/j.ijbiomac.2024.131969.

30 R. Zhang, J. Yang, J. Li, Y. Gao and L. Mao, Modification of the interface of oleogel-hydrogel bigel beads for enhanced stability and prolonged release of bioactives, *Food Chem.*, 2025, **468**, 142448, DOI: 10.1016/j.foodchem.2024.142448.

31 N. Khorshidian, *et al.*, Chitosan-coated alginate microcapsules loaded with herbal galactagogue extract: Formulation optimization and characterization, *Iran. J. Pharm. Res.*, 2019, **18**(3), 1180–1195, DOI: 10.22037/ijpr.2019.1100776.

32 C. Yang, *et al.*, Microencapsulation with chitosan-embedded Houttuynia cordata oil: Integrating antibacterial and antioxidant properties in pork packaging, *Int. J. Biol. Macromol.*, 2025, **314**, 144171, DOI: 10.1016/j.ijbiomac.2025.144171.

33 S. N. Nacer, *et al.*, Phytochemical screening, antioxidant, antibacterial, and antifungal properties of the Cymbopogon citratus methanolic extract, *Pharmacol. Res.*, 2024, **5**, 100094, DOI: 10.1016/j.prenap.2024.100094.